IEEE Access
Multidisciplinary | Rapid Review | Open Access Journal

Received May 17, 2020, accepted June 5, 2020, date of publication June 8, 2020, date of current version June 18, 2020.

Digital Object Identifier 10.1109/ACCESS.2020.3000794

A Comparative Study of Single-Phase AC and Medium Frequency DC Resistance Spot Welding Using Finite Element Modeling

KANG ZHOU[1] AND HUAN LI[2]
[1]School of Mechatronical Engineering, Beijing Institute of Technology, Beijing 100081, China
[2]School of Mechanical Engineering, Yangtze University, Jingzhou 434023, China

Corresponding author: Kang Zhou (zhoukang326@126.com)

This work was supported in part by the National Natural Science Foundation of China under Grant 51605103, and in part by the Beijing Institute of Technology Research Fund Program for Young Scholars under Grant 3020012222008.

ABSTRACT This work deeply explored differences between single-phase AC resistance spot welding (RSW) and three phase medium frequency DC RSW systems. The main difference between the two types of RSW systems was that they used different electrical structures, which led to different energy delivery modes. The RSW operation with former type had a simple but low cost structure, while the latter type had opposite features in these two aspects. In this work, a two-dimensional (2D) finite element (FE) model, which combined characteristics of thermal, electrical, and mechanical fields, was established, and then three modes of input welding currents, which were DC input mode, standard sinusoidal input mode and standard single-phase AC RSW input mode, were delivered into the welding system in the FE model. The three modes of welding currents had strictly the same effective values, and effected the same welding time. By means of iterative calculations between thermal-electrical and mechanical fields, the information of temperature increasing trend, dynamic resistance and electrode displacement under the three input modes were obtained. Some important characteristics about the energy delivery and absorptions, and mechanical properties variations under different welding current input modes which cannot be accurately obtained by actual welding operations had been obtained in this work. Also, other analyses about actual data processing and applications, and mechanical variations of the facilities during the welding process were provided. The work can supple valuable references for actual welding applications.

INDEX TERMS Resistance spot welding, sinusoidal mode, standard single-phase, temperature field, zero welding current.

I. INTRODUCTION

Resistance spot welding(RSW) is widely employed in various industrial occasions [1], such as in bodies and frames of automobiles, trucks, trailers, buses, motor homes, recreational vehicles and railroad passengers cars, as well as office furniture, and many other products [2], [3]. Despite the fact that many advanced spot welding technologies, such as gas tungsten arc spot, laser spot and friction stir spot welding processes, are available in reality, conventional RSW is still the predominant process in sheet metal joining, especially in the manufacturing of automotive industry [4]. Currently, it is estimated that over 90% of assembly works in a car body is completed by RSW process [5]. Hence, this technology is still extensively in practical applications and should be seriously considered in reality.

RSW process is a metal absorbing energy and then melting process [6]. During the process, two or more parent sheet metals are pressed through the upper electrode moving toward to the lower electrode by means of an external electrode force. Then external energy is delivered into welding loads through special electrical structure which includes a step-down welding transformer, and then the welding current goes through the contacted parent sheet metals and the heat energy can be generated from the interface of the contacted sheets. It can be noticed that the energy delivery part is so important because it is responsible for the operational safety and welding quality. In addition, the majority of RSW operations, which mainly

The associate editor coordinating the review of this manuscript and approving it for publication was N. Prabaharan.

cover controls and measurements, are conducted by adjusting the parameters in the energy delivery parts.

In general, there are two distinct types of energy delivery structures employed in reality, which are respectively the single-phase AC structure and three-phase medium frequency DC structure. They have different electrical structures and principles of delivering external electrical energy to melt the welding loads are also so different [7]. Both of two types of energy delivery parts are supplied by common AC power source. The single-phase AC structure uses silicon controlled rectifiers (SCRs) to adjust the electrical energy, and the output is still AC format, but not original standard sinusoidal format; while the three phase medium frequency DC electrical structure uses an H-bridge inverter, which includes four Insulated Gate Bipolar Transistors (IGBTs) and corresponding four diodes, to translate the AC power into approximate DC power to the welding load. It can be noticed that single-phase AC structure is much simpler than that of medium frequency DC structure, and the former structure has low and fixed working frequency, which is the twice of the mains frequency, as well as the output electrical current was not continuous and zero current exists during the process. On the other hand, the later structure has more complicated electrical structure, and the working frequency is so high, which is approximately from 500Hz to 2000Hz and is adjustable, also, the output electrical signal is continuous and the heat energy can be continuously delivered into the welding load. However, the single-phase AC structure has lower price and can be used in many ordinary occasions, while the medium frequency DC structure has higher price and can be employed in some more specialized applications such as the seam welding and aluminum welding in the aerospace industry, where the high power need often requires the use of three-phase rectified welding current [8]. Also, the complicated structure makes the relative contributions much less than that of the single-phase AC structure [9]. Hence, it can be concluded that two types of electrical structures have their special applying areas, based on their different structures and prices, and other relative aspects.

Because consumers have to make choice of using which type of structure can obtain higher efficiency, many scholars and experts paid attentions to the comparison of these two structures. Li *et al* [8] and Alfaro *et al* [10] mainly employed the experimental methods to analyze the differences between the two structures. However, actual experiments cannot guarantee the experimental conditions highly uniform, and some key features and necessary analyses cannot be accurately conducted. Apart from the experimental methods, the former work also used finite element (FE) method to analyze, corresponding conductions and conclusions were not sufficient enough, and the applied conditions were not accurate enough.

In this work, FE method was employed to explore the characteristic differences of these two structures and compare them in various aspects. As a powerful mathematical tool which has more advantages in solving problems with large deformations and can be used to deal with many kinds of engineering problems, especially with complex geometries and materials combinations [11]. Recently, to analyze the RSW phenomena, FE method has been frequently employed to model the RSW operation and many valuable conclusions were driven [12]–[14]. This tool can sufficiently describe the RSW process and obtain many results which cannot be obtained by actual welding operations, so that many in-depth and detailed conclusions can be driven.

However, in previous works which employed FE method to model and analyze the RSW process, accurate and sufficient comparisons between operations using these two electrical structures have not been conducted, also, for the single-phase AC RSW electrical structure, no FE modeling work using precise welding current which included the zero current phase has been published, currently majority of works used approximate input condition without the zero current phase. In this work, the objective is to accurately compare the RSW process respectively using these two structures. To make precise and convinced comparisons, the modeling in this work combined the electrical characteristics, especially for the single-phase AC RSW structure, and then compared the output characteristics obtained from different energy delivery modes. In addition, this work coupled three physical fields, which were respectively thermal, electrical and mechanical fields, and features of temperature variation tendency, dynamic resistance and electrode displacement were employed to reflect the detailed kinds of variations of the workpieces, many characteristics which cannot be precisely obtained by means of actual welding experiments were obtained from this unique operations, and some valuable conclusions were driven to serve the academic researches and practical applications of the RSW system.

II. CHARACTERISTIC OF TWO ELECTRICAL STRUCTRES OF THE RSW OPERATION

As for the characteristics of these two electrical structures, many published contributions have provided detailed introductions. However, in this work, to establish accurate and convinced FE model, some key points should still be seriously considered.

Though the three-phase medium frequency DC electrical structure is more complicated, the electrical output is relatively simple. In current actual application, the operational frequency is so high and the manufacturing and controlling process is so advanced, the actual output of this structure can be considered as a constant during the total energy delivery process. In addition, the effects of magnetic saturation and switch on welding process are so small, hence, it is no necessary to specially present the characteristics in this part.

The single-phase AC electrical structure is relatively simple, however, the output is much more complex than that of medium frequency DC electrical structure. FIGURE 1 shows the schematic of voltage and current waveforms of this electrical structure [9], [15].

In FIGURE 1, α denotes the firing angle of the corresponding SCR in the primary coil of the welding transformer, θ is the conduction angle which denotes the effective range of

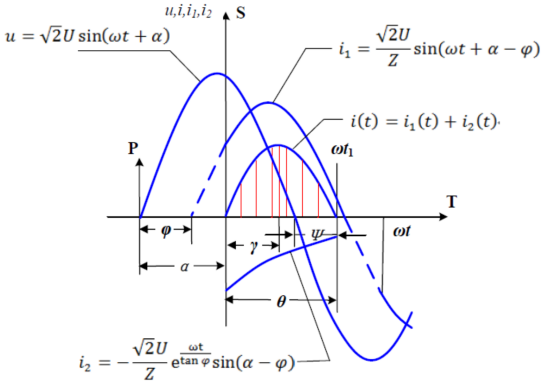

FIGURE 1. Schematic of voltage and current waveforms of single-phase AC RSW machine.

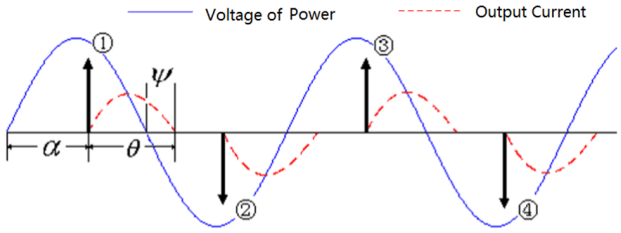

FIGURE 2. Successive waveform of voltage and current.

welding current. Due to existence of inductive components in the system, the output voltage and current in the second coil of the welding transformer have a phase difference, which is marked as ψ and named as phase lag angle. In FIGURE 1, there are two vertical axis P and S, which respectively denote the beginning of voltage in the primary coil and output welding current in the second coil, φ is the power factor angle which denotes the phase difference between input voltage and corresponding current, its mathematical description is $\varphi = \arctan(\omega L/R)$, where L and R respectively denote the equivalent inductance and resistance, ω is the angle frequency, the description is $\omega = 2\pi f$. In addition, γ denotes the angle which corresponds to the peak of the welding current. Under the circumstance, the value of α determines the amount of energy delivered into the welding system, and then generating heat in the welding loads. In other words, all of the currents in the primary and secondary coils are depended by the SCR input firing angle α in the primary coil [16]. Smaller value of α, larger electrode voltage and welding current will be outputted. Moreover, the voltage of welding power source can be denoted as:

$$u(t) = L\frac{di}{dt} + Ri = \sqrt{2}Usin(\omega t + \alpha), \quad (1)$$

and corresponding welding current can be described as:

$$i(t) = \frac{\sqrt{2}U}{Z}[\sin(\omega t + \alpha - \varphi) - e^{-\frac{\omega t}{\tan\varphi}}\sin(\alpha - \varphi)]. \quad (2)$$

where in the FIGURE 1, welding current $i(t)$ is composed of two parts, $i_1(t)$ and $i_2(t)$, which were respectively the forced component and free component of the welding current. It can be noticed that the actual welding current is not successive and one period with zero current exists between any two adjacent control cycles. FIGURE 2 shows four successive cycles during the welding process using this electrical structure [15].

In majority of mathematical models using FE modeling or other tools, the single-phase AC electrical structure used standard sinusoidal format. This was actual an approximate mode which ignored the durations of the zero welding current phase between two successive welding cycles, and was the most commonly-employed energy delivery mode in establishing the mathematical model. In this work, the numerical calculations for AC RSW system respectively employed standard sinusoidal format and standard single-phase AC RSW format showed in equation (2), and then made corresponding comparisons.

III. ESTABLISHING FE MODELS AND MAKING COMPARATIVE CALCULATIONS

To compare the process features and output characteristics of the RSW operations using these two types of electrical structures, numerical calculation using FE model or conductions of actual welding experiments can supply sufficient comparative results. However, it is known that there are many uncertainties and large differences existing in the workpieces, electrodes or other aspects during welding process [17], using actual uniform welding experiments may be difficult to set up. Also, some detailed characteristic samples cannot be accomplished by actual welding experiments. Hence, this work employed numerical calculations to simulate the processes using different welding current input modes. The numerical models can use strictly uniform conditions which were convenient and accurate to make comparisons and can drive more valuable and reliable conclusions.

A. FE MODEL

RSW process couples electrical field, mechanical field and thermal field, in other words, it is a multi-field coupled physical process. In this work, the model was established based on thermal-electrical couple, and then superimposed a calculation of mechanical field. Though the process included other elements which affected the metal melting and phase change, such as electromagnetic stirring and fluid flow behaviors [12], [13], they had limited effects on analyzing the differences of the metal energy absorption, and mechanical properties variation when different modes of input welding currents were employed. Hence, in this work, other elements were not considered, and the work only considered the electrical field, mechanical field, thermal field and their coupled numerical calculation. In general, considering the symmetrical characteristics of the RSW operation, a 1/2 axisymmetric two-dimensional (2D) model was employed in this work, where the horizontal coordinate was x axis and vertical coordinate was y axis. FIGURE 3 shows the FE model established based

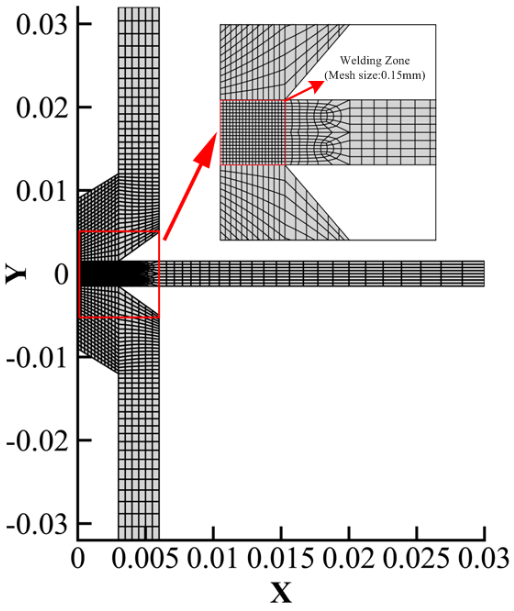

FIGURE 3. 1/2 axisymmetric electric-thermal-mechanical coupled FE model and corresponding meshing presentation.

on commercial software ANSYS 12.1 [18] in the work and corresponding meshing presentation.

The model in this work used a 2D solid 8-node element (PLANE223) to conduct thermal-electrical analysis, and a 2D 8-node surface-to-surface contact element (CONTA172) together with a 2D target segment (TARGE169) to represent the contact pair. Also, to successfully propose a higher strain simulation analysis, a 2D 8-node structural solid (PLANE183) was utilized to conduct structural analysis. In addition, the model in FIGURE 3 included 1824 elements, and the mesh size in the welding zone was 0.15mm. For the thermal-electrical-mechanical analysis for the RSW system, this mesh size was enough to ensure the computational accuracy and reliability, and the grids away from the welding zone were relatively sparser so as to enhance the calculation efficiency. In the model, the maximum aspect ratio was about 1.8, which appeared near the welding zone, and the corresponding mesh size transition was outside the welding zone, where the current density was so low, so the effect on the numerical calculation results was also very low. The quality of the mesh had been checked and no error element or warning was found, by using the mesh check function inside ANSYS. The Jacobian ratios of all the elements were below 30, while the distortion values of all the elements were within the reasonable range. In this work, two workpieces were employed between the upper and lower electrodes, and the width of one workpiece was 1.5 mm, while the length was 30mm. Because the objective of this work was to explore the difference between the processes with two electrical structures, the workpieces used commonly-employed mild steel, which had stable metallurgical characteristics and can be convenient and accurate to analyze. The radius of the electrode was 3 mm, and the material used copper. Some commonly employed key properties of materials were used to serve the FE numerical calculation. The properties included mechanical properties, such as Young's modulus and yield stress, and the physical properties, such as density, thermal conductivity, expansion coefficient and specific heat, as well as the electrical properties, such as the bulk resistivity. The values of majority of these properties changed with temperature both for workpiece and electrode were referred to published contributions [19], [20]. In addition, the tangent modulus of the copper electrode and mild steel were respectively 1800 MPa and 600 MPa, while Poisson's ratios were respectively 0.33 and 0.3 [21]. Because their values had very small variations during the varying range of temperature in this work, the values can be considered as constants during the numerical calculation. The contact algorithm of the numerical calculation was augmented Lagrange method because this method usually led to a better conditioning and was less sensitive to the magnitude of the contact stiffness. Also, the bilinear isotropic (BISO) hardening plasticity model was used in this work. Furthermore, the governing equation of the heat transfer in 2D environment was shown in equation (3):

$$\rho c \frac{\partial T}{\partial \tau} = \frac{\partial}{\partial x}(k\frac{\partial T}{\partial x}) + \frac{\partial}{\partial y}(k\frac{\partial T}{\partial y}) + Q, \tag{3}$$

where T was temperature, τ denoted the time, c was the specific heat capacity, ρ was the density of the material, k was the thermal conductivity and Q was the internal heat. Also, the electrical conduction and mechanical field followed the common formats.

The environmental temperature was 25°C, and the initial electrode force was 5000 N. As for the calculation duration, the medium frequency DC electrical structure outputted a constant welding current and the working frequency was so high, so it is no need to specially consider the duration; however, for the single-phase AC electrical structure, the energy input was counted using sinusoidal wave format, whose frequency is the same as the mains frequency, which was 50Hz in general. The control frequency was twice of the mains frequency. Hence, 100Hz corresponded 0.01s of the welding cycle. Considering the actual RSW operational process and metal characteristic variation during the process, the calculation duration was 0.28s, which should include 14 standard sinusoidal wave format inputs and 28 control cycles. Furthermore, to simulate actual RSW operation, both of the water cooling and air were set based on the actual operation during the process.

In the thermal field and electrical field coupled analysis, the electrical current was applied to the top of the upper electrode and the voltage of the bottom nodes of the lower electrode was set to be 0 volt. The boundary conditions of convection for all surfaces exposed to the air were included, and corresponding heat transfer coefficients were changed with temperature. The convective due to cooling water in the electrode cavity was also included, and the temperature at the interface between electrode and water can be assumed as a

constant value during the RSW process. Latent heat of phase change of the welded joint plates related to enthalpy was considered, and different enthalpy values corresponded to different temperature were used during the calculation. Because the welding process was very short, radiant heat transfer was not considered. In the mechanical analysis, the materials were assumed to follow the von-Mises yield criterion. The pressure was applied to the top of the upper electrode, whereas the bottom nodes of the lower electrode were fixed in the y-direction. A combination of electrical, thermal and mechanical fields was considered as follows: electrical field affected the thermal field and mechanical field including contact area and contact force, the thermal field affected the mechanical field by changing the mechanical properties of materials, and the contact area and contact force affected the thermal field by changing the contact resistance area. Thus, the contact force, contact area and contact resistance were adjusted in every step.

During the process, the thermal-electrical coupled model was first calculated, and then the mechanical model was calculated based on the results obtained from the thermal-electrical coupled model, which were composed of one calculation cycle. The results of this cycle was used for the next calculation cycle. The duration of one calculation cycle corresponded to 0.002s in the welding process, in other word, there were total 140 calculation cycles in the program of this work.

B. THREE MODES OF INPUT WELDING CURRENT

The difference of these two electrical structures was the format of the input welding current. To obtain reliable and accurate comparative results, the uniform input conditions should be strictly set. Three input welding currents were employed in this work, which were constant DC mode, standard sinusoidal mode and standard single-phase AC RSW mode. The second mode, which was standard sinusoidal mode, was chosen as a reference in order to obtain three modes of input welding currents with the same effective values. In this work, the 10000A of peak value of standard sinusoidal mode was chosen. It can be easily obtained that the effective value which corresponded to the DC welding current was 7071A. For the standard single-phase AC RSW mode, two parameters, which were firing angle α and power factor angle φ, should be preliminarily set based on operational characteristics of single-phase AC RSW system. In general, the firing angle can also be marked as firing time according to the translation between time and angle based on the operational frequency. In our system, the operational frequency was 50Hz, which meant that 180° of firing angle can correspond to 0.01s of firing time. Also, the power factor angle should be from 0° to 90°. According to previous researches about the RSW operation with this type of electrical structure [22], [23], the firing time of SCR was about from 0.004 to 0.008, which also corresponded to from 72° to 144° of firing angle, while the power factor angle was about 20° to 50°. In this work, fixed values of these two angles were used, the firing time was set to be 0.45s, which corresponded to 81° of firing angle, and the power factor angle was set to be 40°. Hence, three types of input modes can be obtained. The DC mode was a constant, whose value was 7071A, and the duration was 0.28s. Both of the standard sinusoidal mode and standard single-phase AC RSW mode had 14 cycles, which also corresponded to 0.28s. In addition, the standard single-phase AC RSW mode can calculate corresponding an actual effective value, and then times a coefficient to achieve the same effective values as the other two input modes. FIGURE 4 shows three modes of input welding currents.

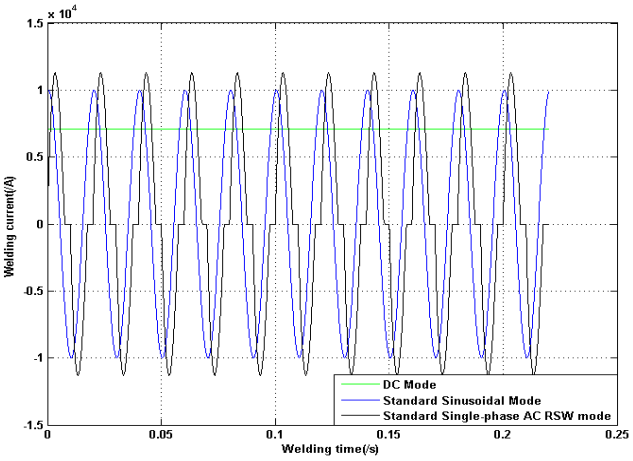

FIGURE 4. Three modes of input welding currents.

It can be seen from FIGURE 4 that DC welding current had the simplest format, which had only one value all over the welding time, the standard sinusoidal mode were composed of sinusoidal lines, and the peak was 10000A. The last was the standard single-phase AC RSW mode which was composed of some inconsecutive lines, in other word, there were zero current between two adjacent control cycles. Because of the existence of the zero current phase, to achieve the same effective value of the welding current, the peak value of each control cycle should be much higher than that of other two modes. The peak value of this mode was 11282A. Hence, the work guaranteed that the three modes of input welding currents had the same effective values, which can make the comparative calculations convinced and valuable.

IV. USING DIFFERENT WELDING CURRENT INPUT MODES TO SIMULATE THE PROCESS AND MAKING COMPARATIVE CALCULATIONS

After established the FE model and obtained three modes of input welding currents, the numerical calculations using different input welding currents can be conducted. In this section, the temperature variation trend, dynamic resistance and electrode displacement can be employed to explore the effects of using different modes of input welding currents on RSW process using the same FE model, and then comparative conclusions and corresponding analyses would be obtained.

A. TEMPERATURE OF THE NUMERICAL CALCULATION RESULTS

First, the final temperature cloud diagrams of three welding current input modes, and corresponding magnified nugget regions were shown in FIGURE 5.

It can be observed that there were very small differences between these three temperature cloud diagrams. Three temperatures were increased respectively from 25°C to 1778°C, 1769°C and 1745°C, as shown in FIGURE 5. Though during the same period, the energy with the same effective values of welding currents delivered into the welding loads, the peak temperature values had a small difference. To clearly observe the temperature situation, the workpieces in three numerical calculations were individually picked and the same scales of the temperature were used. FIGURE 6 showed the comparative temperature cloud diagrams between DC input mode and standard single-phase RSW mode, which respectively corresponded to FIGURE 5 (a) and FIGURE 5(c).

In FIGURE 6, the left side corresponded to the temperature cloud diagram obtained from the DC input mode, while the right side corresponded to the temperature cloud diagram obtained from the standard single-phase RSW mode. It can be seen that though the high-temperature area under DC input mode was a few larger than that under the single-phase AC RSW input mode, the difference was not so remarkable, which coincided the differences of the peak temperatures. In addition, the temperature variation tendencies of two situations were also so approaching. According to FIGURE 6, it can be observed and concluded that the nugget sizes between these two different welding current input modes were so approaching because they were directly and closely related to the temperature variation.

Apart from the temperature cloud diagram, the temperature of one node which located in the interface of two workpieces can also be picked, which was shown in FIGURE 7.

FIGURE 7 showed that in the picked node, which should have the highest temperature, the temperature variations under three different welding current input modes were so approaching. Different input modes might not affect the metal temperature increasing. However, it should be concerned that standard sinosidal and single-phase AC RSW input modes had larger peak values of input welding currents than that of DC input mode, which were respectively 10000A and 11282A versus 7071A, but the corresponding temperature vairations were not much more remarkable than that under the DC input mode. The temperature variations of three curves were in the same limited range, even though under the standard sinosidal mode and standard single-phase AC RSW mode, the magnitude of temperatures had fluctuations, and two fluctuations were so apparaoching and surrouding the curve obtained from DC input mode. To provide much clearer presentation, FIGURE 8 showed the errors of the temperature provided by between DC and single-phase AC RSW input modes.

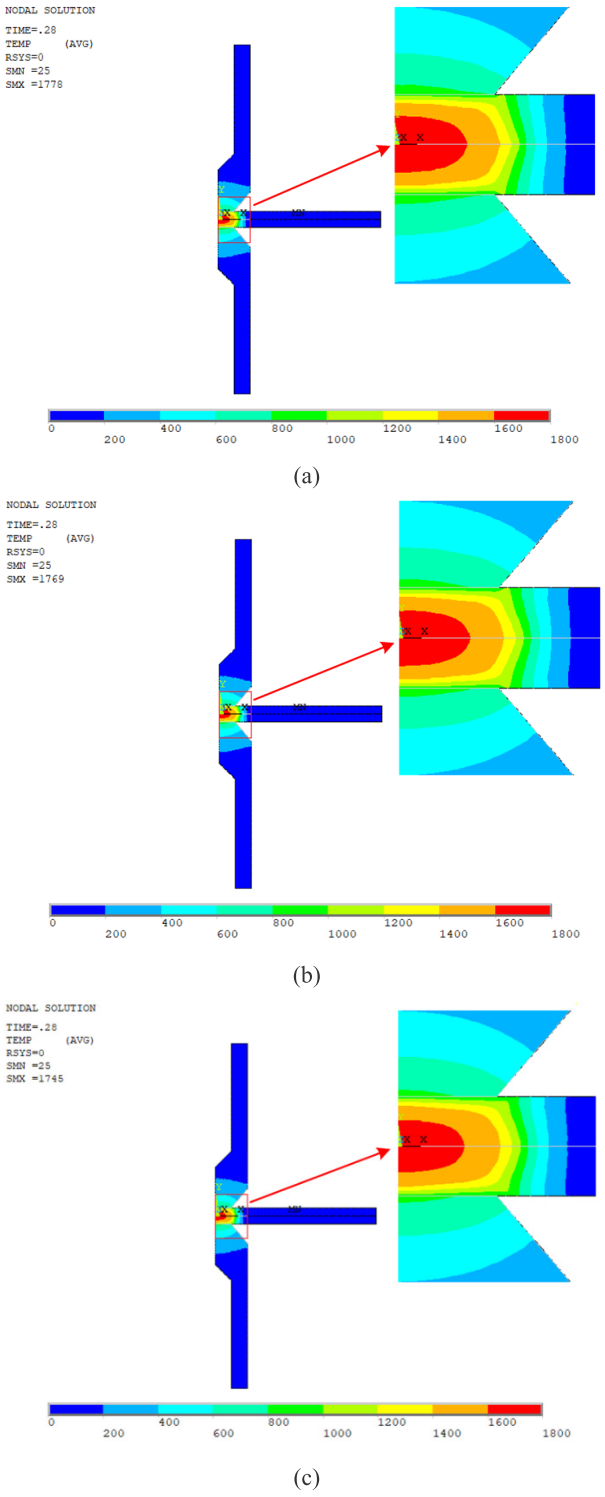

FIGURE 5. Final temperature information using three welding current input moods, (a). DC mode; (b). Standard sinusoidal mode; (c). Standard single-phase RSW mode.

It can be noticed that though the input welding currents had distinct formats, the temperature of the workpieces might had small differences. The zero currents between two adjacent control cycles and severe magnitude variations can only affect

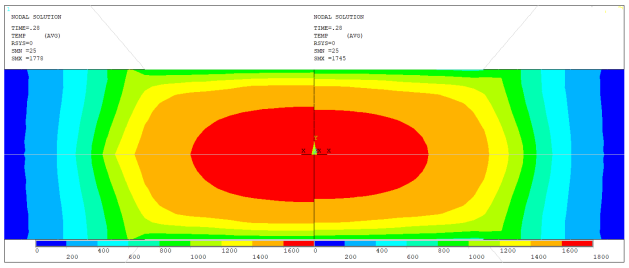

FIGURE 6. Comparative temperature cloud diagram between DC input mode and standard single-phase RSW mode.

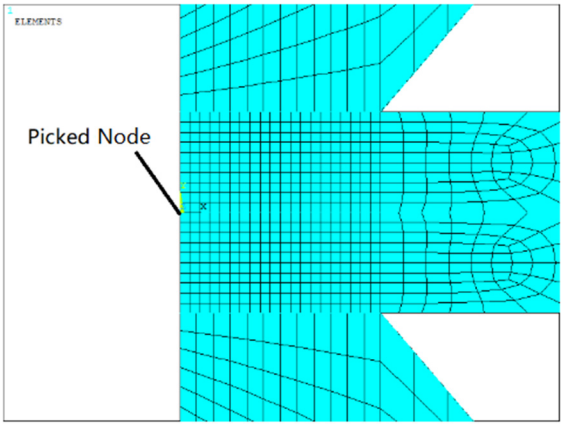

(a)

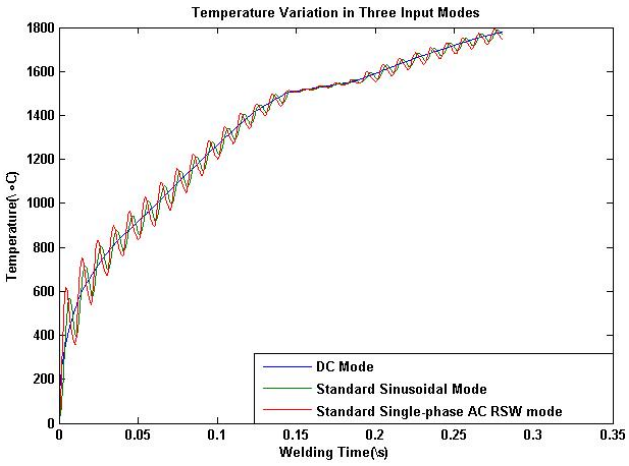

(b)

FIGURE 7. (a). Picked node in the FE model; (b). Temperature variations of the picked node in three input modes.

the energy delivery and absorption a little. At the beginning of the welding pocess, large errors of temperatures were presented becasue the amount of energy which had been absorpted was so little, as the more energy delivered and temperature was much higher, the errors were decreasing. In the middle phase in FIGURE 8, which may be between 0.15s and 0.19s, the errors were much smaller, it was because during that period, the temperature variation was very stable,

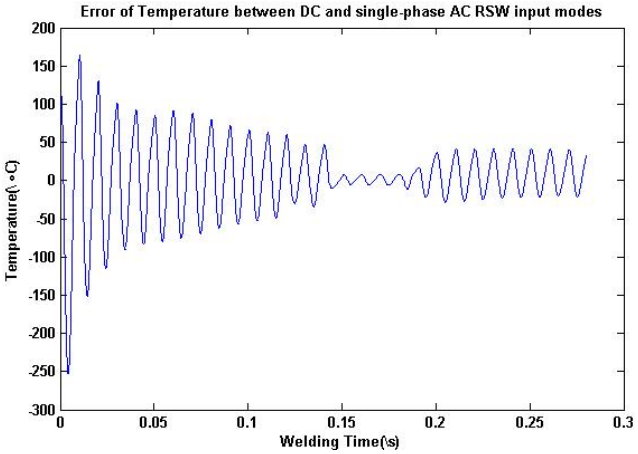

FIGURE 8. Errors of the temperature provided by between DC and single-phase AC RSW input modes.

due to the amount of liquid metals, which were absorbing heat and hindered the temperature decending by phase change, was increasing in a high speed, and this effect was higher than the temperature ascending through other solid metals absorbing heat [24], [25]. Then the errors were more stable than that before above mentioned period, which meant that metal melting and phase transformation process enterred into a relative stable period. As for the error of temperature value, apart from the preceding five control cycles in the single-phase AC RSW input mode, which had large magnitude variations and the overall temperature was so low, the ratio between the largest error value and the DC input welding current was below 10%, and majority ratios were below 5%, which meant that the standard single-phase AC RSW input modes can also effectively increase the temperature and promote the nugget formation and growth, even though the zero current and large magnitudes fluctuation exist.

B. DYNAMIC RESISTANCE OF THE NUMERICAL CALCULATION RESULTS

Apart from the temperature information, other information can also be obtained for making corresponding analyses. The dynamic resistance values were chosen to analyze the variations of workpiece characteristics, because it can adequately reflect the variations of parent sheet metals melting and phase changing during the RSW process [25], [26]. In this work, the dynamic resistance during RSW process with DC input welding current can be conveniently obtained, because the currents were constant during the whole welding process. Each dynamic resistance was obtained using direct quotient between each sampled voltage and constant current values. FIGURE 9 showed the dynamic resistances in this input mode. It can be noticed that the dynamic resistance values were so compacted, which was because the dynamic resistance can be obtained at each sampling point.

When the RSW numerical calculations were conducted under other two types of welding current input modes,

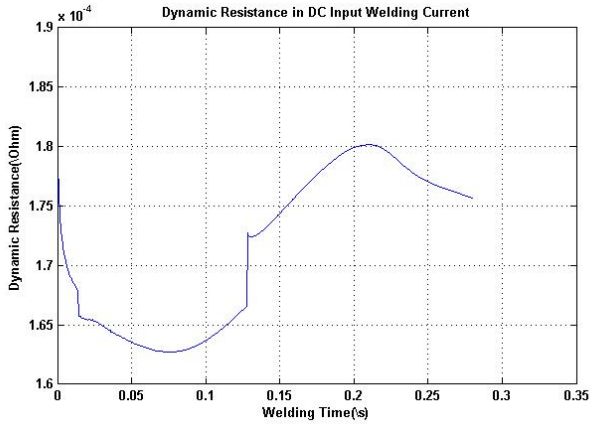

FIGURE 9. Dynamic resistance in DC input welding current.

corresponding dynamic resistances can also be calculated. It must be concerned that no matter the input welding current using standard sinusoidal mode or standard single-phase AC RSW mode, it is difficult to obtain the dynamic resistance at each sample point by direct quotient between electrode voltage and welding current as conducted in DC mode, even under the condition of numerical calculations instead of actual experiments. In our previous work [27], serious test about high-frequency dynamic resistance in single-phase AC RSW can induce large errors. In that work the data was from the actual experiment which may include a lot of sampling and mechanical errors from asymmetry SCR structures. In this work, similar test about direct quotient for high frequency dynamic resistance calculation under numerical calculation was also conducted. The sampled data was obtained from FE model, which ignored the errors which appeared in that previous work, corresponding results of the two input modes were respectively shown in FIGURE 10.

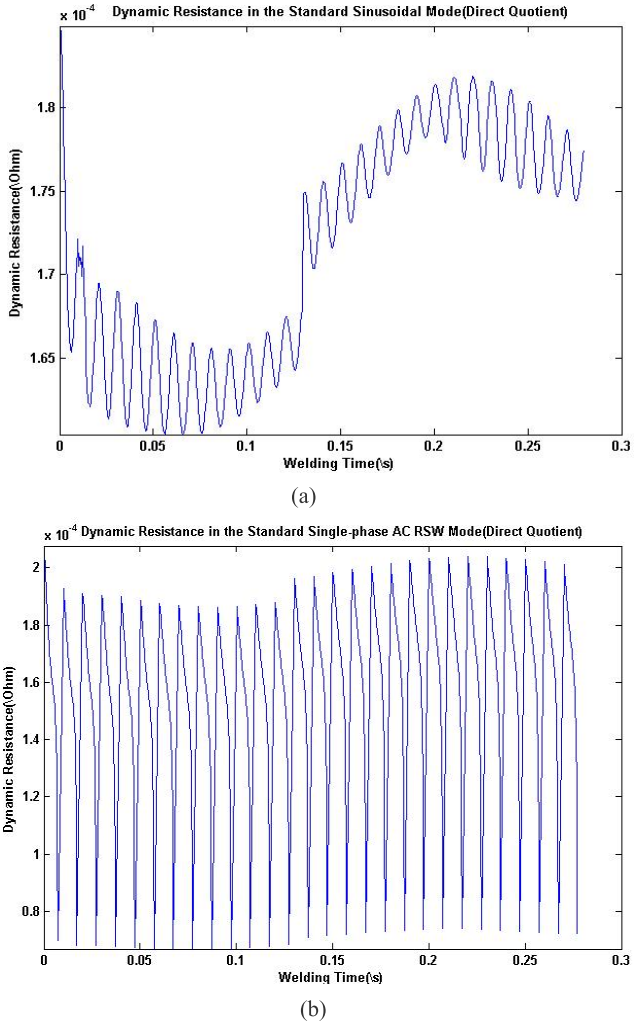

FIGURE 10. Dynamic resistance results obtained from direct quotient, (a). Standard sinusoidal mode, (b). Standard single-phase AC RSW mode.

It can be seen that using direct quotient method can also induce large errors, even though the original voltage and current data were obtained from numerical model instead of actual RSW operations. However, the approximate variation tendency can be detected from these two figures. The dynamic resistance curve in FIGURE 10 (a) was more regular than that in FIGURE 10 (b), which was because there was no zero current interval existing in standard sinusoidal welding current input mode. However, the dynamic resistance in FIGURE 10 (b) can reflect the actual single-phase AC RSW operational condition. Hence, it can be concluded that the unavailability of direct quotient was not totally resulted from mechanical and sample reasons, the data itself may have drawbacks to support direct quotient for obtaining high frequency dynamic resistance. In general, the root mean square (RMS) values of voltage and current values in each welding cycle were be employed to obtain regular dynamic resistance in single-phase AC RSW operation. FIGURE 11 showed the dynamic resistance using RMS values.

Be different from FIGURE 9-10, the lateral axis in FIGURE 11 was labelled using welding control cycle instead of welding time, because the RMS values was only able to be accurately obtained in each control cycle. In this work, one control cycle corresponded to 0.01s. It can be seen that these two welding current input modes can obtain so approximate dynamic resistance curves. Apart from the first two cycles, the two arrays of dynamic resistances had the same variation tendencies and the corresponding values were so approaching. The large differences existed in the first two control cycles may because the initial contact between electrodes and workpieces had large abnormal phenomena, which was why the first two cycle was commonly ignored in many RSW relative analyses, and this phenomenon was also shown in the DC welding current input mode. However, it can be also observed that FIGURE 11 (b) was more regular than that in FIGURE 11 (a), which meant that standard single-phase AC RSW mode was more reasonable than that in standard sinusoidal mode, which was only an approximate in many numerical calculation, especially in the first value in FIGURE 11 (a). It also meant that using standard sinusoidal mode to replace

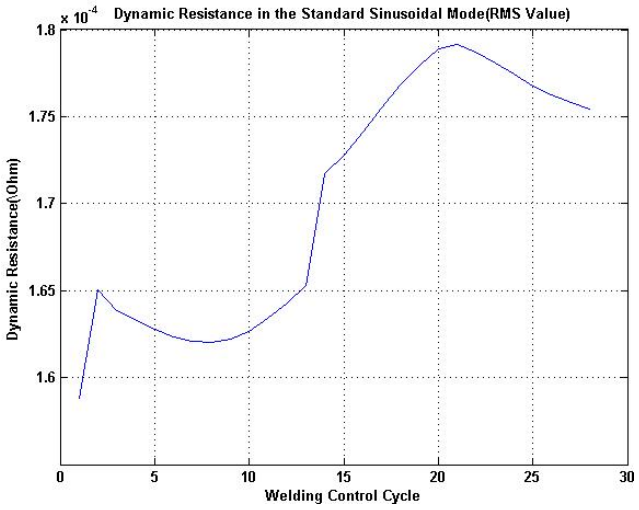

(a)

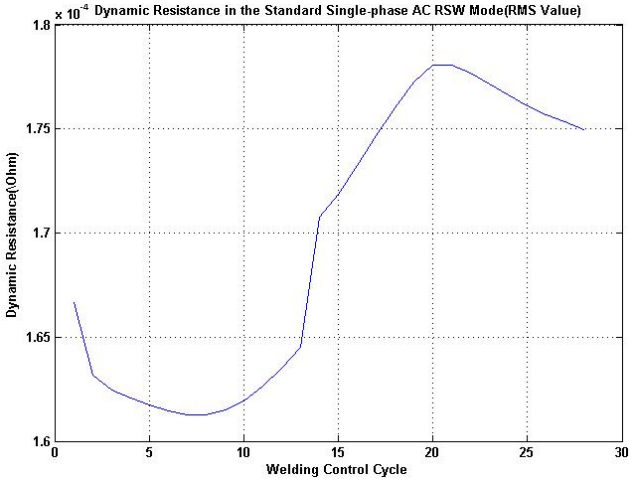

(b)

FIGURE 11. Dynamic resistance results obtained from RMS value, (a). Standard sinusoidal mode, (b). Standard single-phase AC RSW mode.

the standard single-phase AC RSW mode for analyzing the RSW process was reasonable, only except some tiny points.

In addition, it can be observed that the three arrays of dynamic resistances had very approaching variation tendencies, only except the preceding two control cycles, which lasted 0.02s during the process. However, to clearly and seriously explore the variation tendency during the process, detailed data analyses should be conducted. In the analyses of this part, the data obtained under DC and standard single-phase AC RSW input modes after 0.02s of welding time were seriously considered. The minimum and maximum value of dynamic resistances under DC mode were $1.6272 \times 10^{-4}\Omega$ and $1.8016 \times 10^{-4}\Omega$, which corresponded to 0.0762s and 0.2104s of welding time; while the two values under standard single-phase AC RSW input mode were $1.6126 \times 10^{-4}\Omega$ and $1.7807 \times 10^{-4}\Omega$, which corresponded to 8th and 21rd of welding control cycle. It can be seen that these two values corresponded to approximately the same welding time under

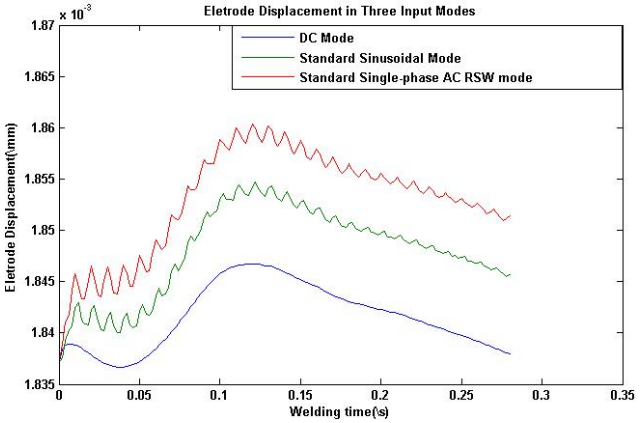

FIGURE 12. Electrode displacement obtained under three different welding current input modes.

the two modes, and differences between minimum and maximum values were respectively $1.5 \times 10^{-6}\Omega$ and $2.1 \times 10^{-6}\Omega$, in addition, the welding times of minimum and maximum values were highly coincided. Hence, combining the profiles shown in FIGURE 9 and FIGURE 11 (b), it can be concluded that these two dynamic resistance curves were highly similar and the two input modes can induce very approaching dynamic resistances.

Moreover, another point should also be concerned. Actually, using DC input mode can directly obtain very accurate, compacted and continuous dynamic resistance data, which was so difficult to be achieved when employed single-phase AC RSW input mode. This merit can significantly benefit for the further analyses for the RSW process, especially in the non-destructive quality estimation or control system design and analyses [28], because more valuable data can be obtained and detailed characteristic analyses can be accomplished, which can induce more useful conclusions.

C. MECHANICAL CHARACTERISTICS OF THE NUMERICAL CALCULATION RESULTS

Apart from thermal and electrical characteristics which were showed respectively by temperature and dynamic resistance mentioned in above two parts, the mechanical characteristics should also be seriously monitored and analyzed is this work. The electrode displacement was chosen to reflect the mechanical characteristic of the RSW process, because it can reflect the physical properties variations and was commonly employed in non-destructive test and online process control [29], [30]. In this FE model, the electrode displacement was exacted under three different welding current input modes. Corresponding figure was showed in FIGURE 12.

It can be observed that the overall trends of above three electrode displacement curves followed the normal variation trend of electrode displacement, which was that the curve can have a small drop first, followed by a raise to a peak, and then have a long time and stable drop, unless an expulsion occurred [6], [29]. Also, the peak of the electrode

displacement occurred before the time when the peak of dynamic resistance appeared. Hence, the curves in FIGURE 12 together with characteristics showed in preceding two characteristics validated the effectiveness and correctness of the established thermal-electrical-mechanical coupled iterative calculation FE model and corresponding numerical calculations. Three curves in FIGURE 12 had very approaching variation tendencies, and the differences between the curves were so small, which meant that the effects of different welding current input modes on mechanical characteristic variations were so small. They had very approaching mechanical characteristics only when the input welding currents had the same effective values during the welding process. However, it must be concerned that three curves were not coincided and had an obvious differences according to the figure, which was not the same as what FIGURE 7 (b) showed. The electrode displacement of the DC mode had the smallest magnitude, followed by the standard sinusoidal input mode, and the standard single-phase AC RSW input mode had the largest magnitude. Though the differences were so tiny, it also meant that the relation between electrode displacement magnitude and stable input welding current was closer than the relation between the magnitude and effective energy delivery. In other words, stable input welding current can induce small electrode displacement magnitude. The magnitude fluctuation of input welding current and zero current existence can increase the overall electrode displacement magnitude. In addition, the electrode displacement magnitude was so sensitive to the input welding current, because varying input welding current can induce varying electrode displacement magnitude. It can be observed that the top two curves have so severe fluctuation, and obviously, the fluctuation of the curve which induced by standard single-phase AC RSW input mode was more severe than that by standard sinusoidal input mode. However, in actual application, these severe fluctuations were difficult to be accurately detected by instrument. This is another advantage which FE model possessed.

Hence, it can be concluded that different formats of input welding currents may also have certain influences on the mechanical characteristic variations, as long as they have the same effective values. The influences were that the electrode displacements had different magnitudes and the variation curves were so sensitive to the magnitude fluctuation of the input welding current.

D. DISCUSSION ABOUT THE COMPARATIVE RESULTS

Though there were other comparative methods during the process, above mentioned temperature increasing, dynamic resistance and electrode displacement can be enough and valuable to be discussed and some meaningful conclusions can be driven. According to the temperature cloud diagram and relative other analyses, the nugget size under DC mode was also a few larger than that under standard single-phase AC RSW mode, which meant that this mode had higher energy absorption efficiency. In addition, the temperature ascending curves under three different welding current input modes may be highly coincided. It meant that the increasing of the metal temperature was attributed to the effective energy delivery, no matter using which type of welding currents. Even though the peak values of welding current under two AC input modes were much higher than that under DC input mode, the temperature increasing under three welding current input modes had a very small difference, which meant that the vibrations of welding current values, especially zero welding currents existed between two adjacent control cycles, only had very limited influence for the heat absorption and temperature increasing of the workpieces, as well as the nugget formation and growth.

In addition, the dynamic resistance curves of DC and standard single-phase AC RSW input modes also had very approximate variation tendencies, including so approaching maximum and minimum values and their corresponding appearing times. Combining that they also had so approximate temperature ascending curves, it meant that the effects of different energy delivery modes on the efficiency of metal absorbing energy and phase changing were low enough, and the most important element was the effective values of the input welding current. Furthermore, it can be noticed that there was a stable period during temperature ascending phase shown in FIGURE 8, which showed that during about from 0.15s to 0.2s, the temperature variation curves under three different modes had the smallest errors, and this particular period was also observed in the dynamic resistance curve. In the two curves showed in FIGURE 11, it can be noticed that peak of dynamic resistance curves also appeared during this period, which validated the effectiveness of model establishment and calculation in this work. Also, the second input mode, which was the standard sinusoidal mode, may induce small errors in calculating the dynamic resistance, which was shown in FIGURE 11 (a). Though this mode was not employed in practice, it was commonly used in numerical calculation to replace the actual single-phase AC RSW mode. It showed that apart from small differences and errors, this replacement was reasonable.

Furthermore, the reasonable electrode displacement curves also further validated the effectiveness of the multi-field coupled FE model by combining the dynamic resistance curves. The results showed that the three electrode displacement curves were so approaching. However, the curves were not coincided as shown in temperature increasing variations, there were tiny differences between curves. The DC input mode had the smallest magnitude variation, while the standard single-phase AC RSW input mode can induce the largest one. In addition, larger varying input welding can induce larger fluctuations of the electrode movements, which can damage the welding machine and corresponding facilities.

Moreover, to achieve the same effective values of different welding current input modes, the standard sinusoidal mode and standard single-phase AC RSW mode should have larger peak value than that of DC mode. Even the peak value of the standard single-phase AC RSW mode was 1.6 times of that under DC mode (11282A versus 7071A). It was known

that high welding current values can induce a lot of disadvantages for the electrical facility. The users should seriously pay attention to this situation. The single-phase AC RSW relative facilities should output higher welding current in order to generate equivalent effects when compared to the medium frequency DC RSW facility, though the latter had more complicated electrical structure and much higher cost.

V. CONCLUSION

This work explored the differences when employed different welding current input modes using FE numerical model. The difference between single-phase AC and medium frequency DC RSW operations was that they had different electrical structures with different welding current input modes. However, systematic exploring the effect of different modes on the temperature increasing and energy absorption was few considered in previous works. Also, majority of numerical calculations for single-phase AC RSW process employed standard sinusoidal input welding current to replace the standard single-phase AC RSW input welding current, however, no detailed analysis had been conducted for this approximate replacement.

The work in this paper established a multi-field coupled FE model which included thermal field, electrical field and mechanical field. For the input welding currents, three welding current input modes, which were DC input mode, standard sinusoidal input mode and standard single-phase AC RSW input mode, were respectively and sequentially employed. Then corresponding numerical calculations were conducted by 140 iterative calculations between thermal–electrical and mechanical models. To guarantee the accuracy and reliability of the comparative analyses, three input modes was set to have strictly the same effective values and the numerical calculations lasted the same welding times. By means of numerical calculations and analyses using FE model, strictly uniform operational conditions can be set and influences from mechanical and other operational reasons can be eliminated, many conductions and phenomena can be driven or obtained, which were difficult to be accurately obtained through actual welding experiments. For the calculation results, according to compare the temperature and dynamic resistance situations, it can be noticed that during the same welding time, the overall temperature cloud diagram had only small differences. Also, according to examine the temperature of one picked node which located in the interface of the two workpiece, the temperature increasing under three input modes followed very approaching trends, so the effects of vibration of the magnitude of input welding current, and the zero welding current existed between adjacent control cycles, on the temperature increasing were so low. Similar phenomenon was also found in analyzing the dynamic resistance curves, three curves had approximately the same variation trends and typical values. Though the dynamic resistances under DC input mode can obtain many continuous and compacted data, while that under two AC input modes only one data can be obtained in each control cycle, it can be observed that the curves were so approaching. This meant that so long as the input welding current had the same effective values, they can have the similar influences on the welding process, no matter in energy absorption or nugget formation and growth.

Also, electrode displacement was obtained through the mechanical field calculation. Three electrode displacement curves under three types of welding current input modes. As the same as the temperature increasing and dynamic resistance, the curves were so approaching, but small differences existed among them and no coincided phenome appeared. The curve obtained from DC input mode was the smoothest variation tendency and lowest magnitude, while the curve under the standard single-phase AC RSW mode had the most severe vibrations and the largest magnitude. Though the differences were small, it meant that the different welding current input modes may affect the mechanical characteristics, which should be seriously considered during the practical applications.

Hence, when the users chose different RSW facilities to conduct the welding operations, the effect of different welding current input modes on the metal phase changing and nugget formation and growth were so low. Above calculation results and corresponding conclusions should be seriously considered. If the facility can guarantee the welding current having the same effective values, they can have very approximate outputs. The users should concern the costs of two types of facilities, and to achieve the same effective values, the welding current in single-phase AC RSW mode should have larger peak value and more severe mechanical variations than those of medium frequency DC mode, also, the AC input modes can induce severe electrode fluctuation during the process. Though some conclusions driven from this numerical calculation were difficult to be verified by actual experiments, in the future more elaborated experiments will be designed and further useful contributions will be supposed to be presented. We hope this work can supply a research foundation for this topic, and can induce more useful and valuable viewpoints in relative areas. Also, this work can help numerical simulation of RSW process choose convenient mode, and is expected to supply reference and enlighten for the RSW and other relative areas, no matter in the academic researches or the actual industrial productions.

REFERENCES

[1] K. Zhou and P. Yao, "Overview of recent advances of process analysis and quality control in resistance spot welding," *Mech. Syst. Signal Process.*, vol. 124, pp. 170–198, Jun. 2019.

[2] X. Sun, Q. Zhang, S. Wang, X. Han, Y. Li, and S. A. David, "Effect of adhesive sealant on resistance spot welding of 301L stainless steel," *J. Manuf. Processes*, vol. 51, pp. 62–72, Mar. 2020.

[3] M. Valaee-Tale, M. Sheikhi, Y. Mazaheri, F. M. Ghaini, and G. R. Usefifar, "Criterion for predicting expulsion in resistance spot welding of steel sheets," *J. Mater. Process. Technol.*, vol. 275, Jan. 2020, Art. no. 116329.

[4] M. Pouranvari and S. P. H. Marashi, "Critical review of automotive steels spot welding: Process, structure and properties," *Sci. Technol. Weld. Joining*, vol. 18, no. 5, pp. 361–403, Jul. 2013.

[5] Y. Li, Z. Lin, Q. Shen, and X. Lai, "Numerical analysis of transport phenomena in resistance spot welding process," *J. Manuf. Sci. Eng.*, vol. 133, no. 3, Jun. 2011, Art. no. 031019.
[6] N. T. Williams and J. D. Parker, "Review of resistance spot welding of steel sheets part 1 modelling and control of weld nugget formation," *Int. Mater. Rev.*, vol. 49, no. 2, pp. 45–75, Apr. 2004.
[7] B. M. Brown, "A comparsion of AC and DC current in the resistance spot welding of automotive steels," *Weld. J.*, vol. 66, no. 1, pp. 18–23, 1987.
[8] W. Li, D. Cerjanec, and G. A. Grzadzinski, "A comparative study of single-phase AC and multiphase DC resistance spot welding," *J. Manuf. Sci. Eng.*, vol. 127, no. 3, pp. 583–589, Aug. 2005.
[9] K. Zhou and P. Yao, "Review of application of the electrical structure in resistance spot welding," *IEEE Access*, vol. 5, pp. 25741–25749, 2017.
[10] S. C. A. Alfaro, J. E. Vargas, M. A. Wolff, and L. O. Vilarinho, "Comparison between AC and MF-DC resistance spot welding by using high speed filming," *J. Achievements Mater. Manuf. Eng.*, vol. 24, no. 1, pp. 333–339, 2007.
[11] W. Mei, "Finite element modeling of resistance spot welding and nugget properties prediction," M.S. thesis, Mech. Eng., Hong Kong Univ. Sci. Technol., Hong Kong, 2009.
[12] Y. B. Li, Z. Q. Lin, S. J. Hu, and G. L. Chen, "Numerical analysis of magnetic fluid dynamics behaviors during resistance spot welding," *J. Appl. Phys.*, vol. 101, no. 5, Mar. 2007, Art. no. 053506.
[13] P. S. Wei and T. H. Wu, "Workpiece property effects on nugget microstructure determined by heat transfer and solidification rate during resistance spot welding," *Int. J. Thermal Sci.*, vol. 86, pp. 421–429, Dec. 2014.
[14] I. Iatcheva, D. Darzhanova, and M. Manilova, "Modeling of electric and heat processes in spot resistance welding of cross-wire steel bars," *Open Phys.*, vol. 16, no. 1, pp. 1–8, Mar. 2018.
[15] K. Zhou and P. Yao, "Simulation of a uniform energy control strategy of single-phase AC resistance spot welding," *Int. J. Adv. Manuf. Technol.*, vol. 94, nos. 5–8, pp. 1771–1779, Feb. 2018.
[16] S. Dhandapani, M. Bridges, and E. Kannatey-Asibu, "Nonlinear electrical modeling for the resistance spot welding process," in *Proc. Amer. Control Conf.*, Jun. 1999, pp. 182–186.
[17] K. Zhou and L. Cai, "On the development of nugget growth model for resistance spot welding," *J. Appl. Phys.*, vol. 115, no. 16, Apr. 2014, Art. no. 164901.
[18] *ANSYS, Inc. Release Notes*, ANSYS. Inc: Canonsburg, PA, USA, 2009.
[19] C. L. Tsai, W. L. Dai, D. W. Dickinson, and J. C. Parritan, "Analysis and development of a real-time control methodology in resistance spot welding," *Weld. J.*, vol. 70, no. 12, pp. 339–351, 1991.
[20] G. Zhong, "Finite element analysis of resistance spot welding process," in *Proc. Chin. Control Decis. Conf.*, Jun. 2009, pp. 5799–5802.
[21] R. Yang, J. Chen, and H. Wang, "Research on finite element modeling of spot weld-bonded joints," (in Chinese), *Chin. J. Automot. Eng.*, vol. 1, no. 5, pp. 448–454, Nov. 2011.
[22] K. Zhou and L. Cai, "Online measuring power factor in AC resistance spot welding," *IEEE Trans. Ind. Electron.*, vol. 61, no. 1, pp. 575–582, Jan. 2014.
[23] K. Zhou and L. Cai, "Study of safety operation of AC resistance spot welding system," *IET Power Electron.*, vol. 7, no. 1, pp. 141–147, Jan. 2014.
[24] D. W. Dickinson, J. E. Franklin, and A. Stanya, "Characterization of spot welding behavior by dynamic electrical parameter monitoring," *Weld. J.*, vol. 59, no. 6, pp. 170–176, Jun. 1980.
[25] W. Tan, Y. Zhou, H. W. Kerr, and S. Lawson, "A study of dynamic resistance during small scale resistance spot welding of thin ni sheets," *J. Phys. D, Appl. Phys.*, vol. 37, no. 14, pp. 1998–2008, Jul. 2004.
[26] K. Zhou, P. Yao, and L. Cai, "Constant current vs. Constant power control in AC resistance spot welding," *J. Mater. Process. Technol.*, vol. 223, pp. 299–304, Sep. 2015.
[27] K. Zhou and L. Cai, "Online nugget diameter control system for resistance spot welding," *Int. J. Adv. Manuf. Technol.*, vol. 68, nos. 9–12, pp. 2571–2588, Oct. 2013.
[28] M. El-Banna, D. Filev, and R. B. Chinnam, "Online qualitative nugget classification by using a linear vector quantization neural network for resistance spot welding," *Int. J. Adv. Manuf. Technol.*, vol. 36, nos. 3–4, pp. 237–248, Mar. 2008.
[29] P. Podržaj, I. Polajnar, J. Diaci, and Z. Karič, "Overview of resistance spot welding control," *Sci. Technol. Weld. Joining*, vol. 13, no. 3, pp. 215–224, Apr. 2008.
[30] H. Zhang, F. Wang, T. Xi, J. Zhao, L. Wang, and W. Gao, "A novel quality evaluation method for resistance spot welding based on the electrode displacement signal and the chernoff faces technique," *Mech. Syst. Signal Process.*, vols. 62–63, pp. 431–443, Oct. 2015.

KANG ZHOU received the bachelor's and master's degrees from the School of Automation, Northwestern Polytechnical University, Xi'an, China, in 2005 and 2008, respectively, and the Ph.D. degree from the Department of Mechanical Engineering from The Hong Kong University of Science and Technology, Hong Kong, in 2013. He is currently an Associate Professor with the School of Mechatronical Engineering, Beijing Institute of Technology. His research interests are in electrical engineering, mechatronics, and intelligent control of welding systems.

HUAN LI received the master's degree from the School of Materials Science and Engineering, Lanzhou University of Technology, Lanzhou, China, in 2012, and the Ph.D. degree from the School of Mechanical and Automotive Engineering, South China University of Technology, Guangzhou, China, in 2018. He is currently a Lecturer with the School of Mechanical Engineering, Yangtze University. His research interests are advanced welding technology and finite element modeling of welding process.